High-affinity DNA-binding Domains of Replication Protein A (RPA) Direct SMARCAL1-dependent Replication Fork Remodeling

Kamakoti P Bhat, Rémy Bétous, David Cortez

THE JOURNAL OF BIOLOGICAL CHEMISTRY VOL. 290, NO. 7, pp. 4110–4117, February 13, 2015

High-affinity DNA-binding Domains of Replication Protein A (RPA) Direct SMARCAL1-dependent Replication Fork Remodeling*

Received for publication, November 19, 2014, and in revised form, December 30, 2014 Published, JBC Papers in Press, December 31, 2014, DOI 10.1074/jbc.M114.627083

Kamakoti P. Bhat[1], **Rémy Bétous, and David Cortez**[2]

From the Department of Biochemistry, Vanderbilt University School of Medicine, Nashville, Tennessee 37232

Background: Replication protein A (RPA) inhibits SMARCAL1 translocation on some substrates but activates it on others.
Results: High-affinity RPA DNA-binding domains (DBDs) are critical to confer substrate specificity to SMARCAL1.
Conclusion: The orientation of the RPA DBDs at the replication fork controls SMARCAL1 substrate specificity.
Significance: The results provide insight into the regulation of DNA translocases by ssDNA-binding proteins.

SMARCAL1 catalyzes replication fork remodeling to maintain genome stability. It is recruited to replication forks via an interaction with replication protein A (RPA), the major ssDNA-binding protein in eukaryotic cells. In addition to directing its localization, RPA also activates SMARCAL1 on some fork substrates but inhibits it on others, thereby conferring substrate specificity to SMARCAL1 fork-remodeling reactions. We investigated the mechanism by which RPA regulates SMARCAL1. Our results indicate that although an interaction between SMARCAL1 and RPA is essential for SMARCAL1 activation, the location of the interacting surface on RPA is not. Counterintuitively, high-affinity DNA binding of RPA DNA-binding domain (DBD) A and DBD-B near the fork junction makes it easier for SMARCAL1 to remodel the fork, which requires removing RPA. We also found that RPA DBD-C and DBD-D are not required for SMARCAL1 regulation. Thus, the orientation of the high-affinity RPA DBDs at forks dictates SMARCAL1 substrate specificity.

Replication is a fundamental process in all organisms and, in humans, involves the accurate and complete duplication of over 6 billion bp of DNA in each cell division cycle. Replication is challenged by DNA lesions, interference from transcription, and difficult-to-replicate sequences, all of which cause replication forks to stall (1). Stalled forks activate the ATR checkpoint kinase, which phosphorylates hundreds of downstream targets to coordinate the replication stress response and promote replication restart and repair (2).

SMARCAL1 is one ATR substrate that travels with the replication fork (3). SMARCAL1 interacts with replication protein A (RPA),[3] the major ssDNA-binding protein (SSB) in human cells, and this interaction is required for SMARCAL1 localization (4–8). SMARCAL1-deficient cells are hypersensitive to replication stress (4–8) and accumulate DNA double-strand breaks catalyzed by the MUS81 nuclease (3). Too much SMARCAL1 activity through either overexpression or lack of restraining phosphorylation by ATR also causes an accumulation of double-strand breaks due to fork cleavage by an SLX4-dependent endonuclease (4, 9). In humans, inherited loss-of-function mutations in *SMARCAL1* cause Schimke immuno-osseous dysplasia, a disease characterized by renal failure, immune deficiencies, cancer susceptibility, and growth defects (10–12).

Biochemically, SMARCAL1 is a DNA translocase that can evict RPA off DNA and anneal complementary strands (13). SMARCAL1 also performs branch migration and fork-remodeling activities (3). Fork remodeling is a proposed mechanism of replication fork stabilization in which the stalled fork is regressed to form a four-way junction called a "chicken foot" (14). This remodeling may promote repair by placing the DNA lesion that stalled the polymerase back into the context of dsDNA. It might also promote lesion bypass through a template-switching mechanism or simply be a mechanism for fork stabilization (14). Once the damage has been bypassed or repaired, the chicken foot is "restored" to a normal fork structure to resume DNA synthesis. RPA confers substrate specificity to SMARCAL1, directing it to regress stalled forks caused by leading-strand lesions and to restore normal forks with lagging-strand ssDNA (15), consistent with a function for SMARCAL1 in promoting genome stability by catalyzing fork remodeling. However, the mechanism by which RPA selectively stimulates SMARCAL1 on certain substrates but inhibits it on others is unknown.

RPA is a heterotrimeric protein with four DNA-binding domains (DBDs) that bind to DNA with a specific orientation (see Fig. 1*A*). These four DBDs do not bind DNA equivalently, with DBD-A having the highest affinity, followed by DBD-B, DBD-C, and DBD-D (16–18). RPA binds DNA, with DBD-A and DBD-B making the initial contacts with 8 nucleotides of DNA (16), and an additional 20 nucleotides are protected when DBD-C and DBD-D bind (17, 19, 20). This 28–30-nucleotide (nt) binding mode causes both the DNA and RPA to undergo major conformational changes and modifies the accessibility of protein-interacting surfaces on RPA (17, 19, 20).

* This work was supported, in whole or in part, by National Institutes of Health Grants R01CA136933 and R01GM160432 (to D. C.).
[1] Supported in part by the Vanderbilt International Scholar Program.
[2] To whom correspondence should be addressed. Tel.: 615-322-8547; Fax: 615-343-0704; E-mail: david.cortez@vanderbilt.edu.
[3] The abbreviations used are: RPA, replication protein A; SSB, ssDNA-binding protein; DBD, DNA-binding domain; nt, nucleotide.

The regulation of DNA translocases by SSBs is an evolutionarily conserved feature of SMARCAL1-related enzymes. *Escherichia coli* RecG and T4 UvsW are regulated by interactions with their SSBs (15, 21, 22). Furthermore, RPA regulates the specificity of many other reactions during replication and repair while being rapidly placed on and taken off DNA (17, 23, 24). The mechanisms underlying this fundamental aspect of DNA biology remain largely unknown. Although RPA can increase the local enzyme concentration to improve reaction rates, this mechanism does not explain how it generates substrate specificity for enzymes such as for SMARCAL1 (15).

In a previous study, we found that RPA regulation of SMARCAL1 is not due to a change in the ability of SMARCAL1 to bind DNA or hydrolyze ATP in the presence of RPA on the different substrates (15). In this study, we examined how RPA directs SMARCAL1 activity on specific substrates by testing two models. In the first model, we hypothesized that the location of the SMARCAL1-binding surface on RPA may be critical for generating substrate specificity. In the second model, we hypothesized that how RPA binds to the ssDNA in relation to the fork junction is important to create an optimal DNA-protein substrate for SMARCAL1. Our data support the second model and provide insights into how SSBs like RPA can generate substrate specificity for DNA translocases.

EXPERIMENTAL PROCEDURES

Cell Culture and Transfection—HEK293T and U2OS cells were cultured in DMEM supplemented with 7.5% fetal bovine serum. HEK293T transfections were performed using PEI (Polysciences, Inc.), and U2OS transfections were done using FuGENE HD (Roche Applied Science).

Recombinant Proteins—FLAG-SMARCAL1 proteins (wild-type, ΔN, and RPA70BD) were purified from HEK293T cells as described previously (3) with the following modifications. Cells transfected with vectors expressing SMARCAL1 were lysed in 150 mM NaCl, 20 mM Tris, 1 mM EDTA, 0.5% Nonidet P-40, 0.2 mM PMSF, 1 mg/ml leupeptin, and 1 mg/ml aprotinin. Following high-speed centrifugation, cleared lysates were incubated with FLAG M2 beads for 4 h at 4 °C. The beads were washed three times with lysis buffer, twice with the LiCl buffer (10 mM HEPES, 0.3 M LiCl, 20% glycerol, 0.01% Triton X-100, 1 mM DTT, 1.5 mM $MgCl_2$, and 0.2 mM PMSF), and once with SMARCAL1 storage buffer (10 mM HEPES, 20% glycerol, 0.01% Triton X-100, 1 mM DTT, 1.5 mM $MgCl_2$, 0.2 mM PMSF, and 0.1 M KCl). The protein was eluted using FLAG peptide at 300 μg/ml. Forms of RPA used included wild-type, DBD-A (AroA, RPA1-F238A,F269A) DBD-B (AroB, RPA1-W361A,F386A), DBD-C (RPA·Zn*, RPA1-C500S,C503S), and FAB-RPA (DBD-F, DBD-A, and DBD-B; RPA-ΔC442) (25, 26). RPA proteins were purified as described previously (25, 26).

DNA Substrate Purification—The oligonucleotides used to create the fork-remodeling substrates were described previously (15). The oligonucleotides used for creating the fork regression substrates with 8-nt gaps are as follows: lead74 (to create an 8-nt lead gap substrate), CGTCGCAGCGACGATCGCACGTCGCGAACAACTTCAGCTGATAGACACGTGGCAATTGCCTACATGTATCCTCA; and lag74 (to create an 8-nt lag gap substrate), TGAGGATACATGTAGGCAATTGCCACGTGTCTATCAGCTGAAGTTGTTCGCGACGTGCGATCGTCGCTGCGACG.

The substrates were purified as described (15) with the exception of the vacuum centrifugation step. Instead, an Amicon Ultra 0.5-ml centrifugal filter (Ultracel, 10,000 nominal molecular weight limit, Millipore) was utilized following the manufacturer's specifications to concentrate the substrate solution.

Electrophoretic Mobility Shift Assays for RPA Binding—^{32}P-Labeled substrate (3 nM) was incubated with different concentrations of RPA in binding buffer containing 40 mM Tris (pH 7.5), 100 mM KCl, 5 mM $MgCl_2$, 100 μg/ml BSA, and 2 mM DTT for 20 min at room temperature. The reactions were separated by electrophoresis on an 8% gel (19:1 polyacrylamide, 1× TBE) at 80 V for 80 min. Gels were dried and quantified using a Molecular Imager FX system (Bio-Rad).

SMARCAL1-DNA Binding Assays—Purified DNA substrate (1 nM) was incubated with increasing concentrations of SMARCAL1 (0.5, 1, and 2 nM) in binding buffer containing 20 mM HEPES, 0.1% Nonidet P-40, 0.1 M KCl, 5 mM $MgCl_2$, 1% glycerol, 0.25 mg/ml BSA, 0.05 M EDTA, and 1 mM DTT for 30 min at room temperature. After adding 15% Ficoll dye to a final concentration of 2.5%, the reactions were separated at 40 V for 200 min on a 5% gel (37.5:1 polyacrylamide, 0.5× TBE) that had been prerun at 4 °C for 30 min. The gels were dried and quantified using the Molecular Imager FX system.

Fork-remodeling Assays—The fork-remodeling assays were performed as described (15). The fork restoration reactions for experiments with RPA mutants DBD-C and FAB were carried out using 1 nM SMARCAL1. The regression reactions and other restoration reactions were carried out using 3 nM SMARCAL1.

Immunofluorescence and Antibodies—For the co-localization experiments, U2OS cells transfected with vectors encoding GFP-SMARCAL1 were plated on coverslips, fixed, and stained using antibodies as described (4).

RESULTS

The Location of the SMARCAL1-interacting Domain on RPA Does Not Dictate Substrate Specificity—RPA activates SMARCAL1 on some fork substrates and inhibits it on others (15). Normal replication forks containing RPA bound to the lagging-strand template are poor substrates for SMARCAL1-catalyzed fork regression, whereas stalled forks with RPA bound to the leading-strand template are good substrates (Fig. 1*B*). Conversely, RPA bound to the chicken foot structures that are created by regression of stalled forks are poor substrates for SMARCAL1-catalyzed fork restoration, whereas chicken foot structures with RPA bound to the nascent leading strand are good substrates. Single-molecule studies indicate that SMARCAL1 moves farther on good substrates than on poor ones (15); however, how RPA dictates this specificity is unknown.

We hypothesized that the selective stimulation of SMARCAL1 is dictated by the orientation of RPA on DNA. Because the four RPA DBDs bind with a 5′ to 3′ polarity (17, 19, 27), the orientation of RPA with respect to the fork junction is different on the stalled fork and the normal fork (Fig. 1*B*). This could translate into a difference in the location of the RPA32C domain that

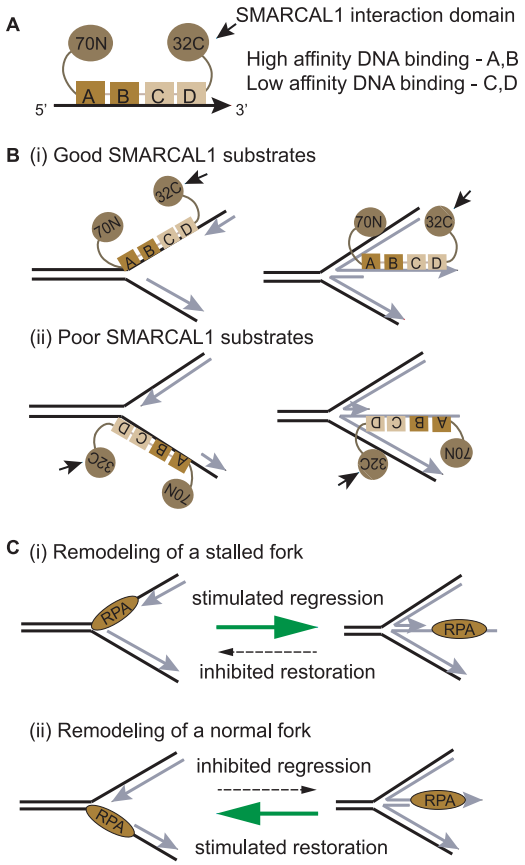

FIGURE 1. **SMARCAL1 is regulated by RPA.** *A*, schematic of RPA bound to ssDNA showing the polarity of the four DBDs and location of the SMARCAL1-interacting domain. *B*, schematic of RPA orientation on the stimulatory and inhibitory substrates. The good SMARCAL1 substrates have the high-affinity DBDs bound close to the fork junction. Also note that the position of RPA32C (the SMARCAL1-interacting domain) may be different on the good and bad SMARCAL1 substrates. The actual spatial locations of the DNA and proteins will be different in the three-dimensional structure of an actual replication fork. *C*, model for repair of stalled replication forks by SMARCAL1. *Panel i*, RPA bound to the leading-strand template stimulates SMARCAL1-catalyzed fork regression. RPA should be present on the leading strand only when the polymerase is stalled. *Panel ii*, RPA bound to the lagging-strand template inhibits SMARCAL1-catalyzed fork regression, thereby preventing aberrant remodeling of an actively elongating fork. However, RPA bound to the nascent leading strand of a reversed fork stimulates SMARCAL1-mediated restoration to a normal fork structure.

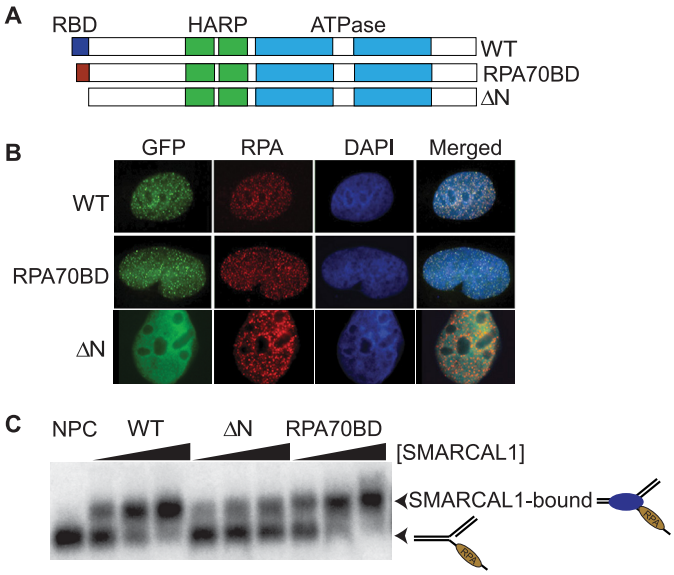

FIGURE 2. **A SMARCAL1 mutant containing an RPA70N-interacting motif binds DNA and is recruited to RPA foci in cells after DNA damage.** *A*, schematic of WT SMARCAL1 (with an RPA32C-interacting motif), SMARCAL1-ΔN (without an RPA-interacting domain), and SMARCAL1-RPA70BD (with an RPA70N-interacting motif). *B*, U2OS cells were transfected with expression vectors for GFP-tagged SMARCAL1, SMARCAL1-RPA70BD, and SMARCAL1-ΔN. The cells were treated with hydroxyurea and imaged for RPA and SMARCAL1. *C*, a model fork substrate was prebound with RPA (so that 100% of the substrate was bound) and incubated with increasing concentrations of the indicated SMARCAL1 protein for 30 min at room temperature. The products were then resolved on a 5% polyacrylamide gel. *NPC*, no-SMARCAL1 protein control.

contacts SMARCAL1 and thereby alters whether RPA stimulates or inhibits SMARCAL1 (Fig. 1, *B* and *C*).

To determine whether the location of the protein-interacting domain on RPA is critical for directing SMARCAL1 to the right substrate, we utilized a SMARCAL1 mutant protein (SMARCAL1-RPA70BD) that interacts with the RPA70N domain instead of the RPA32C domain (28). This mutant substituted an RPA70N-binding motif for the RPA32C-binding motif at the N terminus of SMARCAL1 (Fig. 2*A*). SMARCAL1-RPA70BD bound RPA with similar affinity as wild-type SMARCAL1 (28) and co-localized with RPA in DNA damage foci induced by hydroxyurea (Fig. 2*B*) (4). In contrast, the SMARCAL1-ΔN protein, lacking any RPA-interacting surface, did not localize to stalled forks (Fig. 2*B*) (4). As expected, the DNA-binding ability of SMARCAL1-RPA70BD in the presence of RPA was indistinguishable from that of the wild-type protein (Fig. 2*C*). Because the ΔN protein did not interact with RPA, the DNA-binding ability of SMARCAL1-ΔN in the presence of RPA was slightly reduced, as reported previously (15).

We then tested if the regulation of SMARCAL1 by RPA (15) is retained when SMARCAL1 binds RPA70N instead of RPA32C. RPA modestly stimulated both wild-type SMARCAL1- and SMARCAL1-RPA70BD-catalyzed fork regression when the ssDNA was on the leading-strand template (Fig. 3, *A* and *B*). RPA inhibited SMARCAL1-ΔN-mediated regression as described previously (15), suggesting that RPA acts as a block to SMARCAL1 when there is no interaction between RPA and SMARCAL1. Similarly, RPA stimulated wild-type SMARCAL1 and SMARCAL1-RPA70BD to catalyze fork restoration to the same extent (Fig. 3, *C* and *D*). There was some stimulation of SMARCAL1-ΔN by RPA on the restoration substrate as described previously (15), suggesting an effect of RPA on the DNA substrate that is independent of a physical interaction with SMARCAL1. Also, RPA inhibited fork regression of SMARCAL1-RPA70BD when bound on the lagging-strand template (Fig. 4), similar to its inhibition of wild-type SMARCAL1 and SMARCAL1-ΔN (15), suggesting that inhibition on some substrates is due to a physical block because RPA must be removed during the reaction. This also further confirms that inhibition by RPA is independent of an RPA-SMARCAL1 interaction. Overall, these results support the conclusion that the regulation of SMARCAL1 by RPA is independent of how the two proteins interact because there is no difference in the regulation of wild-type SMARCAL1 and SMARCAL1-RPA70BD.

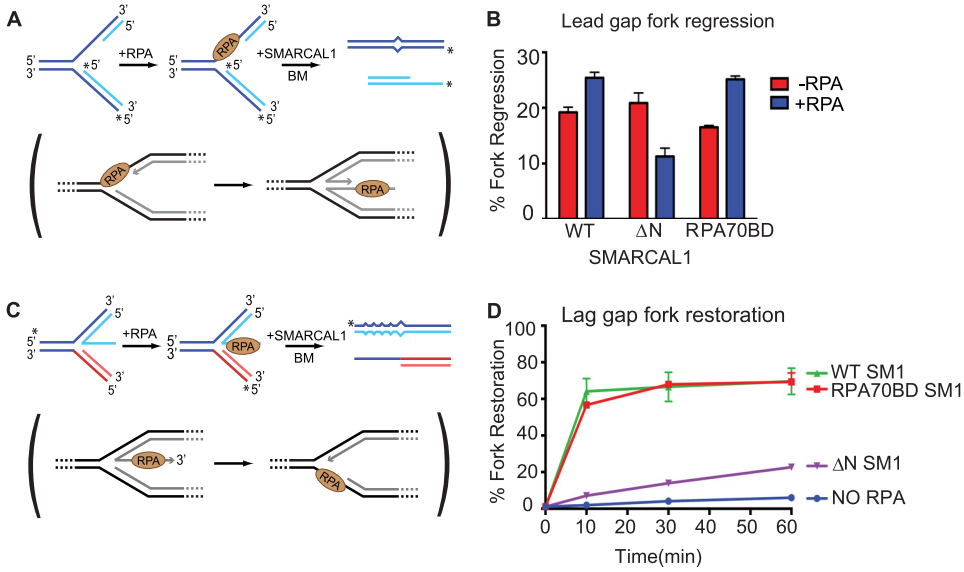

FIGURE 3. **A SMARCAL1 mutant that binds to the RPA70N domain is regulated similarly to wild-type SMARCAL1.** *A* and *C*, schematic of the fork regression and restoration assays, respectively. The ^{32}P-labeled strands are indicated by *asterisks*. The physiological reaction that is mimicked is indicated in *parentheses*. *BM*, branch migration. *B* and *D*, the fork substrates were prebound with RPA and incubated with SMARCAL1 (*SM1*) for 60 min (*B*) or 10, 30, or 60 min (*D*). Products of the reactions were analyzed by native gel electrophoresis. The means ± S.D. from three experiments are shown.

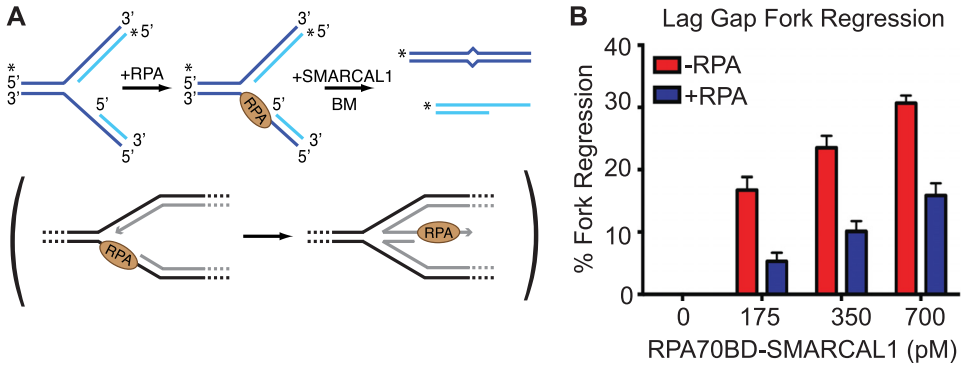

FIGURE 4. **A SMARCAL1 mutant that binds to the RPA70N domain is inhibited by RPA on the normal fork substrate.** *A*, schematic of the lag gap fork regression assay. The ^{32}P-labeled strands are indicated by *asterisks*. The physiological reaction that is mimicked is indicated in *parentheses*. *BM*, branch migration. *B*, the fork substrates were prebound with RPA and incubated with increasing concentrations of SMARCAL1-RPA70BD for 20 min at 30 °C. Products of the reactions were analyzed by native gel electrophoresis. The means ± S.D. from three experiments are shown.

High-affinity RPA-DNA Binding Is Required to Stimulate SMARCAL1—We next hypothesized that the DNA-binding polarity of RPA might be important to regulate SMARCAL1 due to some change imparted on the DNA substrate. In contrast to the highly schematized images in our models, the DNA bound to RPA adopts specific conformations (17, 19, 20, 29), which would make the substrate presented to SMARCAL1 different depending on the orientation of the RPA DBDs. To investigate whether the affinity of RPA-DNA binding is important for stimulating SMARCAL1, we first utilized RPA mutants with altered affinity for DNA due to mutations in either DBD-A or DBD-B (25, 26, 30). These mutations decrease but do not eliminate the affinity of these domains for ssDNA. Wild-type and mutant RPA proteins were added to the DNA substrates at concentrations sufficient to obtain full DNA binding (Fig. 5*A*). The addition of excess wild-type RPA to mimic the higher concentrations of the RPA mutants needed to obtain fully bound substrates did not affect its regulation of SMARCAL1 (data not shown) as reported previously (15).

We then tested if the RPA proteins with mutated DBD-A or DBD-B stimulated SMARCAL1 in the fork-remodeling assays. Because the DBD-A and DBD-B mutations should make it easier for RPA to be removed from the DNA during the reaction, we expected SMARCAL1 to remodel substrates with these mutants more rapidly. However, both the DBD-A and DBD-B mutants displayed a marked decrease in their ability to stimulate SMARCAL1, particularly in the fork restoration assay (Fig. 5, *B–D*). There was still some stimulation compared with the no-RPA control because the mutations did not eliminate binding completely. An RPA protein with mutations in both DBD-A and DBD-B could not be tested because that mutant could not bind the substrates under the conditions used in this assay. Nevertheless, these results indicate that mutations in the high-affinity DBDs that should make it easier for SMARCAL1 to evict RPA actually interfere with the ability of RPA to stimulate SMARCAL1 translocation. However, the RPA DBD-A and DBD-B mutants did not inhibit SMARCAL1 as much as wild-type RPA when bound to the poor substrates (Fig. 5*E*), suggest-

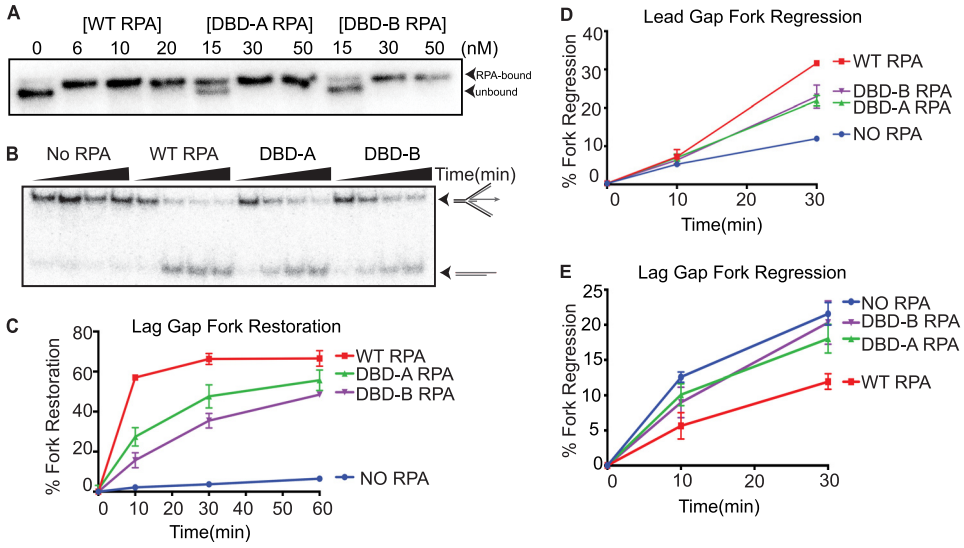

FIGURE 5. **RPA mutants that are defective in binding DNA do not stimulate SMARCAL1 as well as wild-type RPA.** *A*, representative RPA binding assay. The fork regression substrate was incubated with the indicated concentrations of wild-type RPA, DBD-A, or DBD-B for 20 min, and products were analyzed by native gel electrophoresis. The concentrations used in the remodeling assays were 6 nM wild-type RPA and 30 nM DBD-A and DBD-B. *B*, representative autoradiograph of the fork restoration assay with RPA mutants. The substrates and products are indicated. *C–E*, the restoration and regression substrates were prebound with WT RPA, DBD-A, or DBD-B as indicated for 20 min and then incubated with SMARCAL1 for increasing times. The products were analyzed by native gel electrophoresis. The means ± S.D. from three experiments are shown.

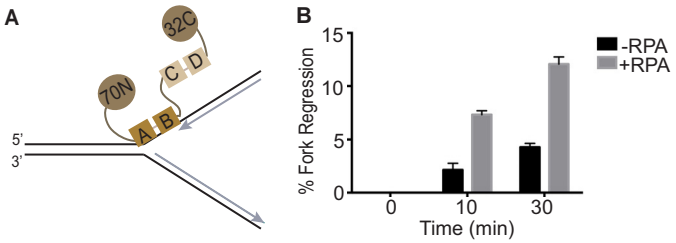

FIGURE 6. **RPA bound to an 8-nt gap is sufficient to stimulate SMARCAL1 regression of a stalled fork.** *A*, schematic of the stalled fork substrate used in the assay. The ssDNA region is limited to 8 nucleotides, allowing the binding of only RPA DBD-A and DBD-B. *B*, the fork substrates were prebound with RPA and incubated with SMARCAL1 for increasing times. Products of the reactions were analyzed by native gel electrophoresis. The means ± S.D. from three experiments are shown.

ing that the inhibitory action of RPA is due to a blocking effect on enzyme movement.

RPA DBD-A and DBD-B Are Sufficient to Regulate SMARCAL1—RPA is removed from ssDNA in two or more steps, with DBD-D and DBD-C coming off first, followed by DBD-B and DBD-A (17, 30, 31). Thus, during the fork-remodeling reactions, there should be an intermediate state where DBD-A and DBD-B are bound to DNA, but DBD-C and DBD-D are not. This could allow SMARCAL1 to access the ssDNA that was bound by DBD-C and DBD-D, and thus allow SMARCAL1 to translocate more efficiently depending on the orientation of the DBDs. To test this idea and if the order of removal of the subunits of RPA off DNA is important, we designed fork substrates with 8-nt ssDNA gap (Fig. 6*A*), sufficient to allow only DBD-A and DBD-B binding to DNA (18, 31–33). Thus, any effect of DBD-C and DBD-D binding the DNA was eliminated. Binding of only RPA DBD-A and DBD-B to ssDNA on the leading-strand template was sufficient to stimulate SMARCAL1-catalyzed regression (Fig. 6*B*). RPA did not stimulate SMARCAL1 when bound to an 8-nt gap on the lagging-strand template (data not shown). The activity of SMARCAL1 on the 8-nt gap substrates was slightly less than on the 30-nt gap substrates. Overall, these experiments suggest that the DNA binding and removal of RPA DBD-C and DBD-D are not essential for regulation of SMARCAL1 and that only DBD-A and DBD-B are critical.

To further test if the DNA binding of DBD-C and DBD-D is dispensable for regulation of SMARCAL1, we utilized an RPA DBD-C mutant that abolished binding of DBD-C and DBD-D to DNA (17, 25, 26, 34) even on a 30-nt ssDNA substrate (Fig. 7*A*). Consistent with the results from the 8-nt ssDNA regression substrates, the RPA DBD-C mutant stimulated SMARCAL1 activity to the same extent as wild-type RPA (Fig. 7*B*), suggesting that DBD-A and DBD-B binding to DNA is sufficient to selectively stimulate SMARCAL1 activity. Because the DBD-C mutant bound DNA with an overall affinity similar to the DBD-A and DBD-B mutants (26), this result also demonstrates that the decrease in the ability of those mutants to stimulate SMARCAL1 is not due to the overall decrease in the DNA affinity of the mutant RPA proteins.

Finally, to confirm that the two high-affinity RPA DBDs are indeed sufficient to stimulate SMARCAL1 when attached to a SMARCAL1-interacting domain, we utilized FAB-RPA, an RPA truncation mutant that has only DBD-A and DBD-B, and the RPA70N protein-interacting domain (26). SMARCAL1 did not interact with the FAB mutant and hence would be expected to behave similarly to SMARCAL1-ΔN. However, SMARCAL1-RPA70BD, the SMARCAL1 mutant that interacted with RPA70N, should have a high level of stimulation with FAB-RPA if the high-affinity DBDs plus a SMARCAL1-interacting surface are sufficient for stimulation. Indeed, wild-type SMARCAL1 behaved like SMARCAL1-ΔN in the presence of FAB-RPA, but SMARCAL1-RPA70BD was stimulated by FAB-RPA to the same extent as wild-type SMARCAL1 by full-length RPA (Fig. 7, *C* and *D*). Thus, an RPA truncation mutant with only the high-affinity DBDs stimulates a SMARCAL1 mutant that interacts with it.

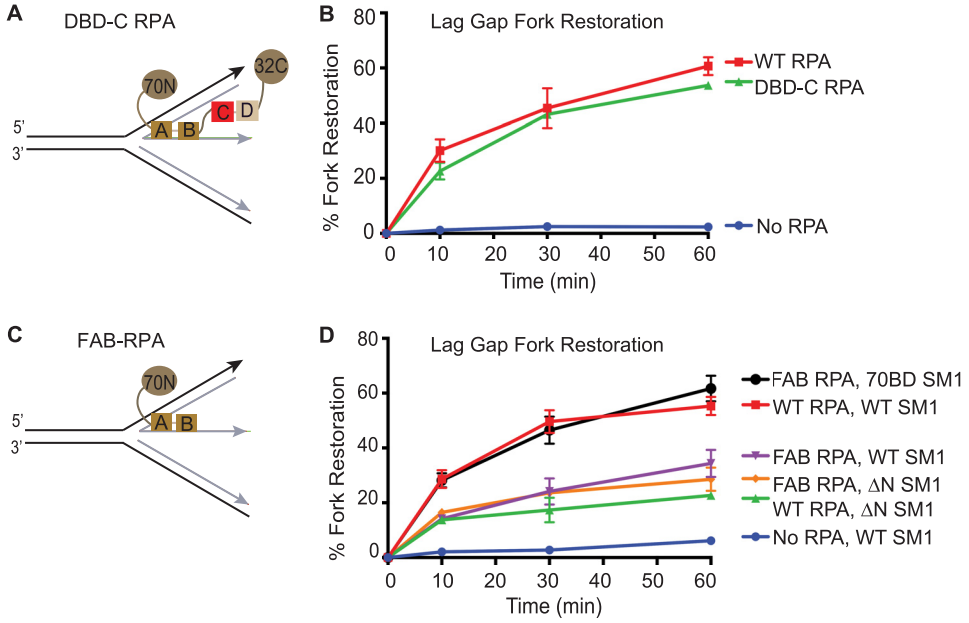

FIGURE 7. **An RPA protein containing only DBD-A, DBD-B, and a SMARCAL1-interacting surface is sufficient to stimulate SMARCAL1.** *A*, schematic of the RPA DBD-C mutant (mutation in DBD-C that abrogates binding to DNA) bound to the substrate. *B*, the fork substrates were prebound with the RPA DBD-C mutant and incubated with 1 nM SMARCAL1 for increasing times. Products of the reactions were analyzed by native gel electrophoresis. The means ± S.D. from three experiments are shown. *C*, schematic of the FAB-RPA protein (RPA that has only DBD-A and DBD-B along with the RPA70N domain) bound to the DNA substrate. *D*, the fork substrates were prebound with FAB-RPA and incubated with the indicated SMARCAL1 (*SM1*) proteins at 1 nM for increasing times. Products of the reactions were analyzed by native gel electrophoresis. The means ± S.D. from three experiments are shown.

DISCUSSION

RPA is an essential regulator of DNA metabolism, serving as both a platform for protein recruitment and a director of enzymatic activities (17, 29). RPA interacts with many DNA translocases and can either stimulate or inhibit enzyme function. However, the mechanism by which it regulates enzymes in addition to increasing their local concentration is largely unknown. Our results reveal insights into the mechanism by which RPA regulates SMARCAL1, a fork-remodeling enzyme, and provide a paradigm for understanding the dynamic nature of RPA-directed DNA metabolism.

Due to the high-affinity binding of RPA to ssDNA, RPA is almost always present when ssDNA forms during DNA replication or repair. Enzymes that translocate on DNA, such as helicases, translocases, and nucleases, must work in the presence of RPA (15, 35–39). Regulation of DNA enzymes by SSBs is a conserved property in all organisms. For example, both *E. coli* SSB and T4 phage gp32 regulate the fork-remodeling proteins RecG and UvsW, respectively (15, 21, 22). However, differences in the structures of the prokaryotic, viral, and eukaryotic SSBs suggest differences in mechanisms.

In some cases, a change in enzyme recruitment or ATPase activity in the presence of the corresponding SSB is important (40–42). However, the regulation of many helicases and translocases such as SMARCAL1 cannot be explained by either mechanism. Also, in more complex examples, RPA stimulates enzymes such as FANCJ and RECQ1 in a strand-specific manner (43). The basis of such regulation is largely not understood.

In the case of SMARCAL1, RPA selectively stimulates regression of a stalled fork and inhibits regression of a normal fork substrate (Fig. 1*C*). It also stimulates SMARCAL1 to restore normal forks while inhibiting its restoration activity when the product looks like a stalled fork. We hypothesized that the polarity of RPA on DNA, which controls the location of the DBDs and the location of the SMARCAL1-interacting surface with respect to the fork junction, conferred substrate specificity. Specifically, we developed two models. The first predicted that the location of the SMARCAL1-interacting surface on RPA is critical for regulation. This model was based on the idea that the RPA protein-interacting domain might be needed as an anchoring point for SMARCAL1 to remove RPA from DNA, with the low-affinity DBD-C and DBD-D being removed first (17, 29, 44). However, our results are inconsistent with this model because a SMARCAL1 mutant that interacts with RPA70N is still regulated by RPA in the same way as wild-type SMARCAL1 that interacts with RPA32C. Also, the crystal structure of RPA bound to DNA and small-angle x-ray scattering and NMR data suggest that RPA bends DNA and that its protein-interacting domains are connected to the DBDs with flexible tethers (19, 20). Thus, the protein-interacting domains could be close in space and incapable of providing firm anchoring points.

In our second model, we hypothesized that the way in which RPA binds replication forks, which is different between the normal fork and the stalled fork due to its asymmetry, is crucial for regulating SMARCAL1. This model predicts that alterations in the RPA DBDs would impact regulation. Indeed, mutations in either of the two high-affinity RPA DBDs caused a marked decrease in the ability of RPA to stimulate SMARCAL1 activity. Furthermore, an RPA protein with only a SMARCAL1-interacting domain and the two high-affinity DBDs is sufficient to activate SMARCAL1. These results are consistent with observations that RPA with mutations in the high-affinity DBDs is defective in DNA repair but can support DNA replication (25).

In summary, these results indicate that the placement of the high-affinity RPA DBDs on DNA substrates dictates SMARCAL1 substrate specificity. Thus, although fork remodeling by SMARCAL1 must happen concurrently with displacement of RPA, some (but not all) mutations that decrease its DNA affinity actually make it more difficult for SMARCAL1 to translocate on the RPA-bound substrate. As might be expected, RPA mutants with lower affinity for DNA make the poor SMARCAL1 substrates better.

RPA binding to DNA is a highly dynamic process, and RPA can diffuse along ssDNA (29, 44, 45). This diffusion of RPA along DNA may destabilize secondary structures to allow access of other proteins to ssDNA (29, 45). RPA diffusion can melt DNA hairpins efficiently when the hairpin is located at the 3′-end. However, when the hairpin is located 5′ to RPA, very little strand melting is observed (45). The high-affinity DBD-A and DBD-B domains are sufficient to induce hairpin destabilization (45). RPA can also promote unwinding of a duplex DNA arm of a synthetic fork in an orientation-specific manner (46). We speculate that RPA might stimulate SMARCAL1 in part by promoting the transient destabilization of the nascent-parental DNA duplex at the fork. This would explain why RPA selectively stimulates SMARCAL1 on some substrates but not others. Alternatively, the selective stimulation of SMARCAL1 could be because RPA induces specific DNA conformations that are more or less conducive to SMARCAL1 DNA translocation depending on RPA orientation with respect to the fork junction. Ultimately, high-resolution structures of enzyme-RPA-DNA complexes will be needed to distinguish between these ideas.

Acknowledgments—We thank Miaw-Sheue Tsai for the production of baculovirus to purify SMARCAL1 proteins (supported by Structural Biology of DNA Repair Machines Grant P01CA092584 from the National Institutes of Health). We also thank Dr. Marc S. Wold (University of Iowa) for all of the purified RPA proteins used in this study.

REFERENCES

1. Zeman, M. K., and Cimprich, K. A. (2014) Causes and consequences of replication stress. *Nat. Cell Biol.* **16,** 2–9
2. Cimprich, K. A., and Cortez, D. (2008) ATR: an essential regulator of genome integrity. *Nat. Rev. Mol. Cell Biol.* **9,** 616–627
3. Bétous, R., Mason, A. C., Rambo, R. P., Bansbach, C. E., Badu-Nkansah, A., Sirbu, B. M., Eichman, B. F., and Cortez, D. (2012) SMARCAL1 catalyzes fork regression and Holliday junction migration to maintain genome stability during DNA replication. *Genes Dev.* **26,** 151–162
4. Bansbach, C. E., Bétous, R., Lovejoy, C. A., Glick, G. G., and Cortez, D. (2009) The annealing helicase SMARCAL1 maintains genome integrity at stalled replication forks. *Genes Dev.* **23,** 2405–2414
5. Yuan, J., Ghosal, G., and Chen, J. (2009) The annealing helicase HARP protects stalled replication forks. *Genes Dev.* **23,** 2394–2399
6. Yusufzai, T., and Kong, X. (2009) The annealing helicase HARP is recruited to DNA repair sites via an interaction with RPA. *Genes Dev.* **23,** 2400–2404
7. Ciccia, A., Bredemeyer, A. L., Sowa, M. E., Terret, M.-E., Jallepalli, P. V., Harper, J. W., and Elledge, S. J. (2009) The SIOD disorder protein SMARCAL1 is an RPA-interacting protein involved in replication fork restart. *Genes Dev.* **23,** 2415–2425
8. Postow, L., Woo, E. M., Chait, B. T., and Funabiki, H. (2009) Identification of SMARCAL1 as a component of the DNA damage response. *J. Biol. Chem.* **284,** 35951–35961
9. Couch, F. B., Bansbach, C. E., Driscoll, R., Luzwick, J. W., Glick, G. G., Bétous, R., Carroll, C. M., Jung, S. Y., Qin, J., Cimprich, K. A., and Cortez, D. (2013) ATR phosphorylates SMARCAL1 to prevent replication fork collapse. *Genes Dev.* **27,** 1610–23
10. Boerkoel, C. F., Takashima, H., John, J., Yan, J., Stankiewicz, P., Rosenbarker, L., André, J.-L., Bogdanovic, R., Burguet, A., Cockfield, S., Cordeiro, I., Fründ, S., Illies, F., Joseph, M., Kaitila, I., Lama, G., Loirat, C., McLeod, D. R., Milford, D. V., Petty, E. M., Rodrigo, F., Saraiva, J. M., Schmidt, B., Smith, G. C., Spranger, J., Stein, A., Thiele, H., Tizard, J., Weksberg, R., Lupski, J. R., and Stockton, D. W. (2002) Mutant chromatin remodeling protein SMARCAL1 causes Schimke immuno-osseous dysplasia. *Nat. Genet.* **30,** 215–220
11. Carroll, C., Badu-Nkansah, A., Hunley, T., Baradaran-Heravi, A., Cortez, D., and Frangoul, H. (2013) Schimke immunoosseous dysplasia associated with undifferentiated carcinoma and a novel SMARCAL1 mutation in a child. *Pediatr. Blood Cancer* **60,** E88–E90
12. Elizondo, L. I., Cho, K. S., Zhang, W., Yan, J., Huang, C., Huang, Y., Choi, K., Sloan, E. A., Deguchi, K., Lou, S., Baradaran-Heravi, A., Takashima, H., Lücke, T., Quiocho, F. A., and Boerkoel, C. F. (2009) Schimke immuno-osseous dysplasia: SMARCAL1 loss-of-function and phenotypic correlation. *J. Med. Genet.* **46,** 49–59
13. Yusufzai, T., and Kadonaga, J. T. (2008) HARP is an ATP-driven annealing helicase. *Science* **322,** 748–750
14. Atkinson, J., and McGlynn, P. (2009) Replication fork reversal and the maintenance of genome stability. *Nucleic Acids Res.* **37,** 3475–3492
15. Bétous, R., Couch, F. B., Mason, A. C., Eichman, B. F., Manosas, M., and Cortez, D. (2013) Substrate-selective repair and restart of replication forks by DNA translocases. *Cell Rep.* **3,** 1958–1969
16. Arunkumar, A. I., Stauffer, M. E., Bochkareva, E., Bochkarev, A., and Chazin, W. J. (2003) Independent and coordinated functions of replication protein A tandem high affinity single-stranded DNA binding domains. *J. Biol. Chem.* **278,** 41077–41082
17. Fanning, E., Klimovich, V., and Nager, A. R. (2006) A dynamic model for replication protein A (RPA) function in DNA processing pathways. *Nucleic Acids Res.* **34,** 4126–4137
18. Wyka, I. M., Dhar, K., Binz, S. K., and Wold, M. S. (2003) Replication protein A interactions with DNA: differential binding of the core domains and analysis of the DNA interaction surface. *Biochemistry* **42,** 12909–12918
19. Brosey, C. A., Yan, C., Tsutakawa, S. E., Heller, W. T., Rambo, R. P., Tainer, J. A., Ivanov, I., and Chazin, W. J. (2013) A new structural framework for integrating replication protein A into DNA processing machinery. *Nucleic Acids Res.* **41,** 2313–2327
20. Fan, J., and Pavletich, N. P. (2012) Structure and conformational change of a replication protein A heterotrimer bound to ssDNA. *Genes Dev.* **26,** 2337–2347
21. Buss, J. A., Kimura, Y., and Bianco, P. R. (2008) RecG interacts directly with SSB: implications for stalled replication fork regression. *Nucleic Acids Res.* **36,** 7029–7042
22. Manosas, M., Perumal, S. K., Bianco, P., Ritort, F., Benkovic, S. J., and Croquette, V. (2013) RecG and UvsW catalyse robust DNA rewinding critical for stalled DNA replication fork rescue. *Nat. Commun.* **4,** 2368
23. Oakley, G. G., and Patrick, S. M. (2010) Replication protein A: directing traffic at the intersection of replication and repair. *Front. Biosci.* **15,** 883–900
24. Borgstahl, G. E. O., Brader, K., Mosel, A., Liu, S., Kremmer, E., Goettsch, K. A., Kolar, C., Nasheuer, H.-P., and Oakley, G. G. (2014) Interplay of DNA damage and cell cycle signaling at the level of human replication protein A. *DNA Repair* **21,** 12–23
25. Hass, C. S., Lam, K., and Wold, M. S. (2012) Repair-specific functions of replication protein A. *J. Biol. Chem.* **287,** 3908–3918
26. Walther, A. P., Gomes, X. V., Lao, Y., Lee, C. G., and Wold, M. S. (1999) Replication protein A interactions with DNA. 1. Functions of the DNA-binding and zinc-finger domains of the 70-kDa subunit. *Biochemistry* **38,** 3963–3973
27. Bochkareva, E., Korolev, S., Lees-Miller, S. P., and Bochkarev, A. (2002) Structure of the RPA trimerization core and its role in the multistep DNA-binding mechanism of RPA. *EMBO J.* **21,** 1855–1863

28. Bétous, R., Glick, G. G., Zhao, R., and Cortez, D. (2013) Identification and characterization of SMARCAL1 protein complexes. *PLoS ONE* **8,** e63149
29. Chen, R., and Wold, M. S. (2014) Replication protein A: single-stranded DNA's first responder: dynamic DNA-interactions allow replication protein A to direct single-strand DNA intermediates into different pathways for synthesis or repair. *BioEssays* **36,** 1156–1161
30. Haring, S. J., Mason, A. C., Binz, S. K., and Wold, M. S. (2008) Cellular functions of human RPA1. Multiple roles of domains in replication, repair, and checkpoints. *J. Biol. Chem.* **283,** 19095–19111
31. Jiang, X., Klimovich, V., Arunkumar, A. I., Hysinger, E. B., Wang, Y., Ott, R. D., Guler, G. D., Weiner, B., Chazin, W. J., and Fanning, E. (2006) Structural mechanism of RPA loading on DNA during activation of a simple pre-replication complex. *EMBO J.* **25,** 5516–5526
32. Kolpashchikov, D. M., Khodyreva, S. N., Khlimankov, D. Y., Wold, M. S., Favre, A., and Lavrik, O. I. (2001) Polarity of human replication protein A binding to DNA. *Nucleic Acids Res.* **29,** 373–379
33. Lavrik, O. I., Kolpashchikov, D. M., Weisshart, K., Nasheuer, H.-P., Khodyreva, S. N., and Favre, A. (1999) RPA subunit arrangement near the 3′-end of the primer is modulated by the length of the template strand and cooperative protein interactions. *Nucleic Acids Res.* **27,** 4235–4240
34. Bochkareva, E., Korolev, S., and Bochkarev, A. (2000) The role for zinc in replication protein A. *J. Biol. Chem.* **275,** 27332–27338
35. Doherty, K. M., Sommers, J. A., Gray, M. D., Lee, J. W., von Kobbe, C., Thoma, N. H., Kureekattil, R. P., Kenny, M. K., and Brosh, R. M., Jr. (2005) Physical and functional mapping of the replication protein a interaction domain of the Werner and Bloom syndrome helicases. *J. Biol. Chem.* **280,** 29494–29505
36. Brosh, R. M., Jr., Li, J. L., Kenny, M. K., Karow, J. K., Cooper, M. P., Kureekattil, R. P., Hickson, I. D., and Bohr, V. A. (2000) Replication protein A physically interacts with the Bloom's syndrome protein and stimulates its helicase activity. *J. Biol. Chem.* **275,** 23500–23508
37. Sommers, J. A., Banerjee, T., Hinds, T., Wan, B., Wold, M. S., Lei, M., and Brosh, R. M., Jr. (2014) Novel function of the Fanconi anemia group J or RECQ1 helicase to disrupt protein-DNA complexes in a replication protein A-stimulated manner. *J. Biol. Chem.* **289,** 19928–19941
38. Machwe, A., Lozada, E., Wold, M. S., Li, G.-M., and Orren, D. K. (2011) Molecular cooperation between the Werner syndrome protein and replication protein A in relation to replication fork blockage. *J. Biol. Chem.* **286,** 3497–3508
39. Shen, J. C., Gray, M. D., Oshima, J., and Loeb, L. A. (1998) Characterization of Werner syndrome protein DNA helicase activity: directionality, substrate dependence and stimulation by replication protein A. *Nucleic Acids Res.* **26,** 2879–2885
40. Abd Wahab, S., Choi, M., and Bianco, P. R. (2013) Characterization of the ATPase activity of RecG and RuvAB proteins on model fork structures reveals insight into stalled DNA replication fork repair. *J. Biol. Chem.* **288,** 26397–26409
41. Shereda, R. D., Bernstein, D. A., and Keck, J. L. (2007) A central role for SSB in *Escherichia coli* RecQ DNA helicase function. *J. Biol. Chem.* **282,** 19247–19258
42. Ranalli, T. A., DeMott, M. S., and Bambara, R. A. (2002) Mechanism underlying replication protein a stimulation of DNA ligase I. *J. Biol. Chem.* **277,** 1719–1727
43. Suhasini, A. N., Sommers, J. A., Mason, A. C., Voloshin, O. N., Camerini-Otero, R. D., Wold, M. S., and Brosh, R. M., Jr. (2009) FANCJ helicase uniquely senses oxidative base damage in either strand of duplex DNA and is stimulated by replication protein A to unwind the damaged DNA substrate in a strand-specific manner. *J. Biol. Chem.* **284,** 18458–18470
44. Gibb, B., Ye, L. F., Gergoudis, S. C., Kwon, Y., Niu, H., Sung, P., and Greene, E. C. (2014) Concentration-dependent exchange of replication protein A on single-stranded DNA revealed by single-molecule imaging. *PLoS ONE* **9,** e87922
45. Nguyen, B., Sokoloski, J., Galletto, R., Elson, E. L., Wold, M. S., and Lohman, T. M. (2014) Diffusion of human replication protein A along single-stranded DNA. *J. Mol. Biol.* **426,** 3246–3261
46. Delagoutte, E., Heneman-Masurel, A., and Baldacci, G. (2011) Single-stranded DNA binding proteins unwind the newly synthesized double-stranded DNA of model miniforks. *Biochemistry* **50,** 932–944